

Baryon density and magnetic field effects on chaos in a $Q\bar{Q}$ system at finite temperature

Nicola Losacco

Istituto Nazionale di Fisica Nucleare, Sezione di Bari, Via Orabona 4, I-70126 Bari, Italy
Dipartimento Interateneo di Fisica “M. Merlin”, Università e Politecnico di Bari,
via Orabona 4, 70126 Bari, Italy

Abstract

Baryon density and magnetic field effect on chaos for the holographic dual of a $Q\bar{Q}$ system at finite temperature is studied. A string in an AdS Reissner–Nordstrom background, and in a metric with magnetic field near the black-hole horizon is considered and small time-dependent perturbations of the static configurations are investigated. The proximity to the horizon induces chaos, which is softened increasing the chemical potential or the magnetic field. A background geometry including the effect of a dilaton is also examined. The Maldacena, Shenker, and Stanford bound on the Lyapunov exponents characterizing the perturbations is satisfied for finite baryon chemical potential and magnetic field and when the dilaton is included in the metric.

1 Introduction

The aim of these studies [1, 2] is to analyze the effects of baryon density and magnetic field on the chaotic behavior of a suspended string in a gravitational background. The works follow the tests, carried out using holographic methods, of the Maldacena-Shenker-Stanford (MSS) bound [3]. The bound, conjectured to be universal, states that, under general conditions, for a thermal quantum system at temperature T some out-of-time-ordered correlation functions involving Hermitian operators which characterize the system have an exponential time dependence in determined time intervals. The dependence is characterized by the exponent λ , for which a bound (in units where $\hbar = 1$ and $k_B = 1$) can be obtained:

$$\lambda \leq 2\pi T. \tag{1}$$

The correlation functions quantify quantum chaos. They are the thermal expectation values of the squared commutator of two Hermitian operators at a time separation t , that allow to determine the effect of one operator on measurements of the other one at a later time.

The MSS bound should be satisfied by a set of systems called fast “scramblers”. The possibility to apply holographic methods to test the bound is supported by the observation that in nature the black holes (BH) are the fastest scramblers: the time needed for a system near a BH horizon to lose information depends logarithmically on the number of the system degrees of freedom [4, 5]. Connections between chaotic quantum systems and gravity have been investigated in [6–10]. In a holographic framework, a relation has been worked out between the size of the operators of the quantum theory on the boundary, which are involved in the temporal evolution of the perturbation, and the momentum of a particle falling in the bulk [11, 12].

To test the MSS bound (1) through holographic methods, the quantum system is conjectured to be a $4d$ boundary theory dual to an AdS_5 gravity theory with a black hole [13–15]. Several investigations are described in [16–20]. Most of the studies analyze the dynamics of a string hanging in the bulk with endpoints on the boundary, which is the holographic dual of a static quark-antiquark pair [21–24]. To quantify the chaotic dynamics of such systems, the Lyapunov exponent λ , characterizing the chaotic behavior of the fluctuations around the static string configuration is evaluated [25–27]. In the work [28] the bound has been generalized to a quantum system in a thermal ensemble and a global symmetry. In the case of QCD, the global symmetry can be related to the conservation of the baryon number. The generalization in [28] relaxes the MSS bound:

$$\lambda \leq \frac{2\pi T}{1 - \left| \frac{\mu}{\mu_c} \right|}, \quad (2)$$

where μ is the chemical potential related to the global symmetry, and μ_c a critical value above which the thermodynamic ensemble is not defined. The inequality (2) is conjectured for $\mu \ll \mu_c$. This means that systems that satisfy the bound (2) could violate the MSS one.

In this review a general approach to study the chaotic behavior of such systems is presented. Two applications of the procedure are analyzed. The first one aims to test the generalized bound, considering the role of a $U(1)$ global symmetry connected to the conservation of the baryon number. In such case, a dual metric can be identified with the AdS Reissner-Nordstrom (RN) metric with a charged black hole. We can use this background for testing Eq.(2). The second case analyzes the impact of an external magnetic field on the chaotic behaviour of the string. The magnetic field is relevant in different contexts, including heavy-ion collisions or condensed matter problems such as the Quantum Hall Effect and superconductivity at high temperatures. A general gravity dual for such systems is presented in [29–34]. The backreaction of an external magnetic field modifies the geometry of the $5d$ spacetime, the metric of which is determined by the Einstein equations. As a result, an anisotropy is introduced in the spatial directions. Moreover, in a finite temperature system the relation between the position of the black hole horizon, the source of chaos in the $5d$ geometry, and temperature, involved in the MSS relation in

the boundary theory, is modified by the magnetic field.

2 String profile in the gravitational background

We are interested in the gravity dual of a strongly coupled $Q\bar{Q}$ pair in a general thermodynamic background at finite temperature. The hanging string is described by the functions $r(t, \ell)$ and $x_i(t, \ell)$, in an asymptotically AdS_5 geometry with a black hole. The endpoints of the string are on the AdS boundary $r \rightarrow \infty$. (t, ℓ) are the worldsheet coordinates, with ℓ the proper distance measured along the string, Fig. 1.

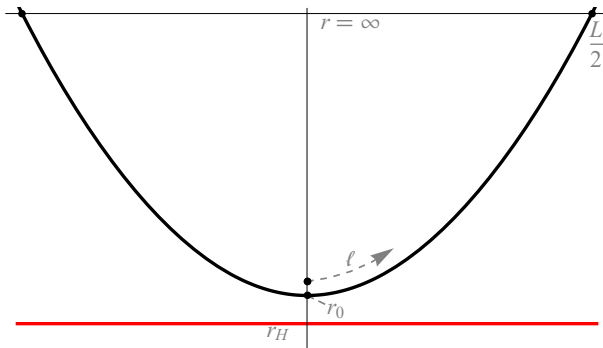


Figure 1: Profile of a static string for the $Q\bar{Q}$ system. r_0 is the position of the tip of the string, r_H the position of the horizon, L the distance between the end points on the boundary.

The line element for a generic 5 dimensional diagonal metric can be expressed as

$$ds^2 = g_{tt}dt^2 + g_{11}(dx^1)^2 + g_{22}(dx^2)^2 + g_{33}(dx^3)^2 + g_{rr}dr^2. \quad (3)$$

The string dynamics is governed by the Nambu-Goto (NG) action:

$$\mathcal{S} = -\frac{1}{2\pi\alpha'} \int dt d\ell \sqrt{-h}, \quad (4)$$

where α' is the string tension and h the determinant of the induced metric $h_{ij} = g_{MN} \frac{\partial X^M}{\partial \xi_i} \frac{\partial X^N}{\partial \xi_j}$, with $\xi_{i,j}$ the worldsheet coordinates and g the metric tensor. In the static case the action reads:

$$\mathcal{S} = -\frac{T}{2\pi\alpha'} \int d\ell \sqrt{|g_{tt}g_{ii}\dot{x}_i^2 + g_{tt}g_{rr}\dot{r}^2|}, \quad (5)$$

where \dot{x}_i denotes the derivative with respect to ℓ . x_i is a cyclic coordinate, so its conjugate momentum

$$\frac{\partial \mathcal{L}}{\partial \dot{x}_i} = -\frac{T}{2\pi\alpha'} \frac{|g_{tt}g_{ii}\dot{x}_i|}{\sqrt{|g_{tt}g_{ii}\dot{x}_i^2 + |g_{tt}g_{rr}\dot{r}^2|}} \quad (6)$$

is a constant of motion. Denoting with $r(\ell = 0) = r_0$ the position of the tip of the string in the bulk, i.e. the point where $\left. \frac{dr}{dx_i} \right|_{\ell=0} = 0$, we have:

$$\frac{\sqrt{|g_{tt}|g_{ii}\dot{x}_i}}{\sqrt{g_{ii}\dot{x}_i^2 + g_{rr}\dot{r}^2}} = \sqrt{|g_{tt}|g_{ii}} \Big|_{\ell=0}. \quad (7)$$

Moreover, from the condition

$$d\ell^2 = g_{ii} dx_i^2 + g_{rr} dr^2 \quad (8)$$

the equations determining the string profile can be obtained:

$$\dot{x} = \pm \frac{\sqrt{-g_{tt}(r_0)g_{ii}(r_0)}}{\sqrt{-g_{tt}g_{ii}}} \quad (9)$$

$$\dot{r} = \pm \frac{\sqrt{-g_{tt}g_{ii} + g_{tt}(r_0)g_{ii}(r_0)}}{\sqrt{-g_{tt}g_{ii}g_{rr}}}. \quad (10)$$

We set the string endpoints lying on the AdS₅ boundary at $x_i = \pm L/2$. The minimum value r_0 of the coordinate r is reached at $x_i = 0$ (or $\ell = 0$). L and r_0 are related, since

$$L = 2 \int_{r_0}^{\infty} dr \left(\frac{g_{ii}(r)}{g_{rr}(r)} \left(\frac{g_{tt}(r)g_{ii}(r)}{g_{tt}(r_0)g_{ii}(r_0)} - 1 \right) \right)^{-\frac{1}{2}}. \quad (11)$$

Therefore, the static string configuration depends on r_0 or L . Choosing different configurations, it is possible to probe the effect of the closeness of the BH horizon on the chaotic behaviour of the string. As shown in Ref. [1] the proximity to the horizon enhances the chaotic behaviour, hence we choose an unstable configuration near the horizon as starting point to perturb and study the dynamics of the fluctuation.

3 Perturbing the static solution

The chaotic dynamics can be studied by perturbing the static string configuration near the black hole horizon. The perturbation is chosen to be orthogonal in each point of the string, and described by the coordinate ℓ in the $r - x$ plane [1, 25]. The perturbation is depicted in Fig. 2. Considering the unit vector $n^M = (0, n^x, 0, 0, n^r)$ orthogonal to t^M , we have:

$$g_{rr}(r) (n^r)^2 + g_{xx}(r) (n^x)^2 = 1 \quad (12)$$

$$\dot{r}(\ell) g_{rr}(r) n^r + \dot{x}(\ell) g_{xx}(r) n^x = 0. \quad (13)$$

For an outward perturbation as in Fig. 2 the solution for the components n^x and n^r is

$$n^x(\ell) = \sqrt{\frac{g_{rr}}{g_{xx}}} \dot{r}(\ell) \quad , \quad n^r(\ell) = -\sqrt{\frac{g_{xx}}{g_{rr}}} \dot{x}(\ell) \quad . \quad (14)$$

The time-dependent perturbation $\xi(t, \ell)$ modifies r and x :

$$\begin{aligned} r(t, \ell) &= r_{BG}(\ell) + \xi(t, \ell) n^r(\ell) , \\ x(t, \ell) &= x_{BG}(\ell) + \xi(t, \ell) n^x(\ell) , \end{aligned} \quad (15)$$

where $r_{BG}(\ell)$ and $x_{BG}(\ell)$ are the static solutions obtained integrating Eqs. (9) and (10).

The dynamics of the small perturbation can be analyzed expanding the metric function around the static solution $r_{BG}(\ell)$ to the third order in $\xi(t, \ell)$. To this order the NG action comprises a quadratic and a cubic term. The quadratic term has the form:

$$S^{(2)} = \frac{1}{2\pi\alpha'} \int dt \int_{-\infty}^{\infty} d\ell \left(C_{tt} \dot{\xi}^2 + C_{\ell\ell} \xi'^2 + C_{00} \xi^2 \right) . \quad (16)$$

C_{tt} , $C_{\ell\ell}$ and C_{00} depend on ℓ and on the parameters of the metric. The equation of motion from the action (16) is

$$C_{tt} \ddot{\xi} + \partial_\ell \left(C_{\ell\ell} \dot{\xi} \right) - C_{00} \xi = 0 . \quad (17)$$

Factorizing $\xi(t, \ell) = \xi(\ell) e^{i\omega t}$ it corresponds to the Sturm-Liouville equation

$$\partial_\ell \left(C_{\ell\ell} \dot{\xi} \right) - C_{00} \xi = \omega^2 C_{tt} \xi , \quad (18)$$

with $W(\ell) = -C_{tt}(\ell)$ the weight function. Eq. (18) can be solved for different values of the parameters characterizing the metric. The two lowest eigenvalues ω_0^2 and ω_1^2 , with

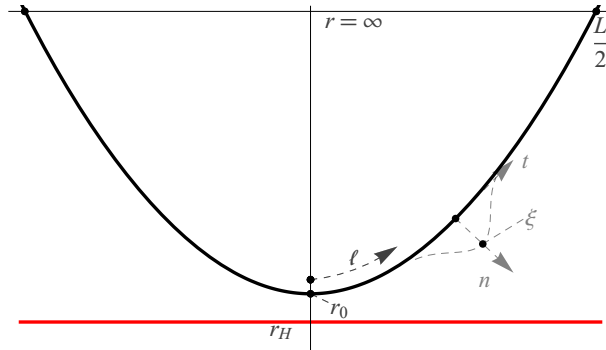


Figure 2: Static string profile and perturbation $\xi(t, \ell)$ along the direction orthogonal to the string in each point with coordinate ℓ .

the corresponding eigenfunctions $\xi(\ell) = e_0(\ell)$ and $\xi(\ell) = e_1(\ell)$ can be obtained. The third order terms in ξ in the action give us information on the chaotic behaviour. Up to a surface term, the expression is

$$S^{(3)} = \frac{1}{2\pi\alpha'} \int dt \int_{-\infty}^{\infty} d\ell \left\{ D_0 \xi^3 + D_1 \xi \dot{\xi}^2 + D_2 \xi \dot{\xi}^2 \right\}, \quad (19)$$

with $D_{0,1,2}$ functions of ℓ . Expanding the perturbation in terms of the first two eigenfunctions $e_0(\ell)$ and $e_1(\ell)$,

$$\xi(t, \ell) = c_0(t) e_0(\ell) + c_1(t) e_1(\ell), \quad (20)$$

the time dependence of the perturbation is encoded in the coefficients $c_0(t)$ and $c_1(t)$. With this form of $\xi(t, \ell)$ we have

$$\begin{aligned} S^{(3)} = & \\ & \frac{1}{2\pi\alpha'} \int dt \int_{-\infty}^{\infty} d\ell \left[\left(D_0 e_0^3 + D_1 e_0 e_0^2 \right) c_0^3(t) + \left(3D_0 e_0 e_1^2 + D_1 (2\dot{e}_0 e_1 \dot{e}_1 + e_0 \dot{e}_1^2) \right) c_0 c_1^2 \right. \\ & \left. + D_2 \left(e_0 e_1^2 c_0 \dot{c}_1^2 + e_0^3 e_1^2 c_0 \dot{c}_0^2 + 2e_0 e_1^2 \dot{c}_0 c_1 \dot{c}_1 \right) \right]. \end{aligned} \quad (21)$$

The action for $c_0(t)$ and $c_1(t)$ is obtained by $S^{(2)} + S^{(3)}$, integrating over ℓ :

$$S^{(2)} + S^{(3)} = \frac{1}{2\pi\alpha'} \int dt \left[\sum_{n=0,1} (\dot{c}_n^2 - \omega_n^2 c_n^2) + K_1 c_0^3 + K_2 c_0 c_1^2 + K_3 c_0 \dot{c}_0^2 + K_4 c_0 \dot{c}_1^2 + K_5 \dot{c}_0 c_1 \dot{c}_1 \right]. \quad (22)$$

The coefficients $K_{1,\dots,5}$ depend on r_0 and on the parameters of the metric. In general the potential described by Eq. (22) has a trap for the unstable string configurations. We are interested in the motion of c_0 and c_1 in the trap. In some regions of the potential the kinetic term is negative. As shown in [1, 25], it is useful to replace $c_{0,1} \rightarrow \tilde{c}_{0,1}$ in the action, with $c_0 = \tilde{c}_0 + \alpha_1 \tilde{c}_0^2 + \alpha_2 \tilde{c}_1^2$ and $c_1 = \tilde{c}_1 + \alpha_3 \tilde{c}_0 \tilde{c}_1$, neglecting $\mathcal{O}(\tilde{c}_i^4)$ terms, setting the constants α_i ensuring the positivity of the kinetic term. This replacement stretches the potential and stabilizes the time evolution of the system. The dynamics is not affected, and a chaotic behaviour shows up in the transformed system.

4 Geometry

The procedure can now be applied to specific cases. Interesting systems could be a $Q\bar{Q}$ pair in a finite temperature and baryon density background, and the pair in a constant and uniform magnetic field at finite temperature. The first one would allow us to test (2), and therefore to relax the MSS bound in the presence of a global symmetry, and the other is relevant in different phenomenological contexts. We need to specify the dual metric of the systems solving Einstein equations with suitable boundary conditions.

4.1 Finite baryon density

Consider a Lagrangian of a quantum field theory with a $U(1)$ gauge symmetry and a Dirac fermion charged under this symmetry,

$$\mathcal{L} = i\bar{\psi}\gamma^\mu D_\mu\psi - \frac{1}{4g^2}F^{\mu\nu}F_{\mu\nu}, \quad (23)$$

with the covariant derivative $D_\mu = \partial_\mu + iA_\mu$. A chemical potential can be introduced considering a non-vanishing background field

$$A_0 = \mu, \quad A_i = 0 \quad (i = 1, \dots, 3). \quad (24)$$

This generates a potential of the form

$$V = -\mu \psi^\dagger\psi. \quad (25)$$

Since $\psi^\dagger\psi = \hat{N}$ is the number operator, μ is the chemical potential by definition: it represents the change in energy of the system when a particle is added.

We are interested in finding the *AdS* gravity dual of this system. In general the gravity action describing the 5-dimensional asymptotic AdS space and the gauge field is given by

$$S = \int d^5x \sqrt{-G} \left[\frac{1}{2k^2} (\mathcal{R} - 2\Lambda) - \frac{1}{4g^2} F_{MN}F^{MN} \right], \quad (26)$$

where $2k^2$ is proportional to the five-dimensional Newton constant and g^2 is a five-dimensional gauge coupling constant. In the *AdS*₅ space, the cosmological constant is given by $\Lambda = -6/L^2$, where L is the radius of the *AdS* space. The equations of motion of this system are

$$\begin{aligned} \mathcal{R}_{MN} - \frac{1}{2}G_{MN}\mathcal{R} + G_{MN}\Lambda &= \frac{k^2}{g^2} \left(F_{MP}F^P{}_N - \frac{1}{4}G_{MN}F_{PQ}F^{PQ} \right), \\ 0 &= \partial_M \sqrt{-G} G^{MP} G^{NQ} F_{PQ}, \end{aligned} \quad (27)$$

the Einstein equations and the Maxwell ones. Knowing the five-dimensional gauge field A^M in the AdS space, Eq. (27) gives the metric of the space. To recover the gauge theory at the boundary of the AdS space we set

$$A_0(x^\mu, z) = \mu - Qz^2, \quad A_i = A_4 = 0 \quad (i = 1, 2, 3), \quad (28)$$

where $z = 1/r$ is the bulk coordinate in the Fefferman-Graham coordinate system. The line element of a 5-dimensional asymptotic AdS spacetime reads

$$ds^2 = \frac{L^2}{z^2} \left(-f(z) dt^2 + d\mathbf{x}^2 + \frac{1}{f(z)} dz^2 \right), \quad (29)$$

and the boundary is $z = 0$.

Solving Eq. (27) we obtain the Reissner-Nordstrom AdS black-hole

$$f(z) = 1 - mz^4 + q^2z^6, \quad (30)$$

where m is the mass of the black-hole and q is its charge. Introducing Eq. (28) and Eq. (30) in Eq. (27) and evaluating it at the boundary $z = 0$ we obtain a relation between q and Q

$$q^2 = \frac{2k^2}{3g^2L^2} Q^2. \quad (31)$$

In the AdS/QCD context, the gravitation constant $2k^2$ and the 5-dimensional coupling constant g^2 are related to the rank of the gauge group N_c and the number of flavors N_f in QCD [35]

$$\frac{1}{2k^2} = \frac{N_c^2}{8\pi^2L^3} \quad \text{and} \quad \frac{1}{g^2} = \frac{N_cN_f}{4\pi^2L}, \quad (32)$$

therefore, Eq. (32) can be written as

$$q = \sqrt{\frac{2}{3} \frac{N_f}{N_c}} Q. \quad (33)$$

The RN black-hole has two horizons identified by the solutions of

$$f(z_h) = 1 - mz_h^4 + q^2z_h^6 = 0. \quad (34)$$

We can write the mass of the black-hole as a function of the outer horizon and of its charge:

$$m = \frac{1}{z_h^4} + q^2z_h^2. \quad (35)$$

To show the relation between the charge q and the chemical potential μ we can observe that to have a regular norm $A^M(x^\mu, z) A_M(x^\mu, z) \equiv G^{00} A_0 A_0$, $A^0(x^\mu, z)$ should vanish at the outer horizon therefore

$$A^0(x^\mu, z_h) = \mu - Q z_h^2 = 0. \quad (36)$$

This gives

$$Q = \frac{\mu}{z_h^2}. \quad (37)$$

Using Eq. (33) we have the relation between the charge of the black-hole and the chemical potential

$$q = \sqrt{\frac{2 N_f}{3 N_c}} \frac{\mu}{z_h^2}. \quad (38)$$

Inserting Eq. (35) and Eq. (38) in Eq. (30) we obtain:

$$\begin{aligned} f(z) &= 1 - \frac{z^4}{z_h^4} - \left(\frac{2 N_f}{3 N_c}\right) \frac{\mu^2 z^4}{z_h^2} + \left(\frac{2 N_f}{3 N_c}\right) \frac{z^6 \mu^2}{z_h^4} \\ &= 1 - \frac{z^4}{z_h^4} - \frac{\mu^2 z^4}{z_h^2} + \frac{z^6 \mu^2}{z_h^4}, \end{aligned} \quad (39)$$

where the coefficient $\frac{2 N_f}{3 N_c}$ is absorbed in the definition of μ^2 . Returning to the r coordinates we obtain the RN metric function

$$f(r) = 1 - \frac{r^4}{r_h^4} - \frac{\mu^2 r^2}{r^4} + \frac{r^4 \mu^2}{r^6}. \quad (40)$$

The line element is obtained from Eq. (29) setting $L = 1$

$$ds^2 = -f(r) r^2 dt^2 + r^2 d\mathbf{x}^2 + \frac{1}{r^2 f(r)} dr^2, \quad (41)$$

and the Hawking temperature T is

$$T = \frac{r_h}{\pi} \left| 1 - \frac{\mu^2}{2r_h^2} \right|. \quad (42)$$

4.2 Magnetic field

A magnetic field is introduced in the holographic framework by a $U(1)$ gauge field F_{MN} which modifies the $5d$ geometry. The metric is determined solving the Einstein equations:

$$R_{MN} - \frac{1}{2}g_{MN}(R + 12) - T_{MN} = 0 \quad (43)$$

with the $5d$ stress-energy tensor

$$T_{MN} = 2(g^{AB}F_{MA}F_{NB} - \frac{1}{4}g_{MN}F^2). \quad (44)$$

For a constant magnetic field B in the x_3 direction F is given by $F = B dx^1 \wedge dx^2$, hence the only nonvanishing components are $F_{12} = -F_{21} = B$. The Einstein equations have been solved perturbatively in the low- B and high temperature limits in Refs. [36–38]. The result for the line element, having the general expression

$$ds^2 = g_{tt}dt^2 + g_{11}(dx^1)^2 + g_{22}(dx^2)^2 + g_{33}(dx^3)^2 + g_{rr}dr^2 \quad (45)$$

with $r > r_h$, reads:

$$g_{tt} = -r^2 f(r), \quad g_{11} = g_{22} = r^2 h(r), \quad g_{33} = r^2 q(r), \quad g_{rr} = \frac{1}{r^2 f(r)}. \quad (46)$$

The metric functions are expressed as [38]

$$f(r) = 1 - \frac{2B^2}{3r^4} \log r + \frac{f_4}{r^4} \quad (47)$$

$$q(r) = 1 - \frac{2B^2}{3r^4} \log r \quad (48)$$

$$h(r) = 1 + \frac{B^2}{3r^4} \log r. \quad (49)$$

The magnetic field breaks rotational invariance, hence $g_{22} \neq g_{33}$. The geometry has a horizon, the position of which r_h is found requiring $f(r_h) = 0$. This gives $f_4 = -r_h^4 + \frac{2}{3}B^2 \log(r_h)$ and the blackening function $f(r)$

$$f(r) = 1 - \frac{r_h^4}{r^4} - \frac{2B^2}{3r^4} \log \frac{r}{r_h}. \quad (50)$$

The Hawking temperature T depends on the magnetic field:

$$T = \frac{r_h}{\pi} \left(1 - \frac{B^2}{6r_h^4} \right). \quad (51)$$

The metric given in terms of the functions (47)-(49) is obtained for large bulk coordinate r and low B , and it is important to reckon the minimum value of r and the largest value of B for which it is a good approximation of Eqs. (43),(44) and (46). This metric can be compared to the one obtained by numerical solution of the Einstein equation. The comparison shows that the deviation in using the approximated metric are small and can be safely used.

5 Poincaré sections and Lyapunov exponents

We can apply the procedure discussed in section 2 and 3. We start by choosing a static string configuration fixing the tip position of the string. We consider the energy of the string configuration as a function of r_0 , Fig. 3, and observe that the the energy has a peak near the BH horizon. The configurations closer to the horizon are unstable, and the effect of chaos is enanched. $r_0 = 1.1$ is chosen as the tip position for the static configuration for both metrics.

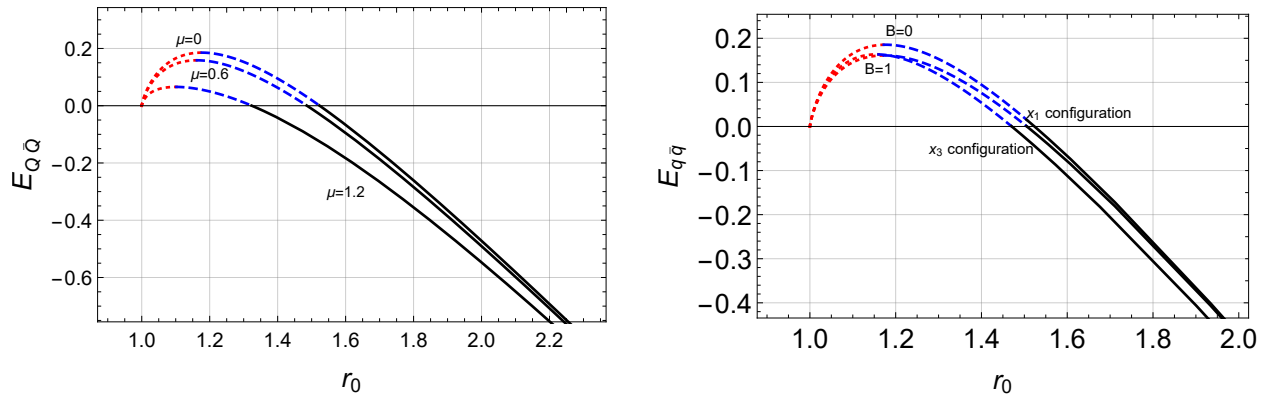


Figure 3: Energy of the string configuration as a function of r_0 for different values of chemical potential μ (left) and magnetic field B (right). The maximum divides the unstable configurations (red dotted line) from the metastable (blue dashed line) and stable (solid black line) ones.

We now perturb the static string, and from Eq. (22) we obtain the dynamics of the fluctuation through the functions $c_0(t)$ and $c_1(t)$. The onset of chaos is displayed by the Poincaré sections. We construct the sections defined by $\tilde{c}_1(t) = 0$ and $\dot{\tilde{c}}_1(t) \geq 0$ for bounded orbits within the trap in the potential. Setting $r_h = 1$ and $r_0 = 1.1$ for both metrics, we obtain the sections Fig. 4,5 for different values of μ and B . For \tilde{c}_0 near zero the orbits are scattered points which depend on the initial conditions. Increasing μ or B the points in the sections arrange in more regular paths, showing that the effect of switching on the magnetic field, or the interaction with a baryon reservoir is to mitigate the chaotic behavior.

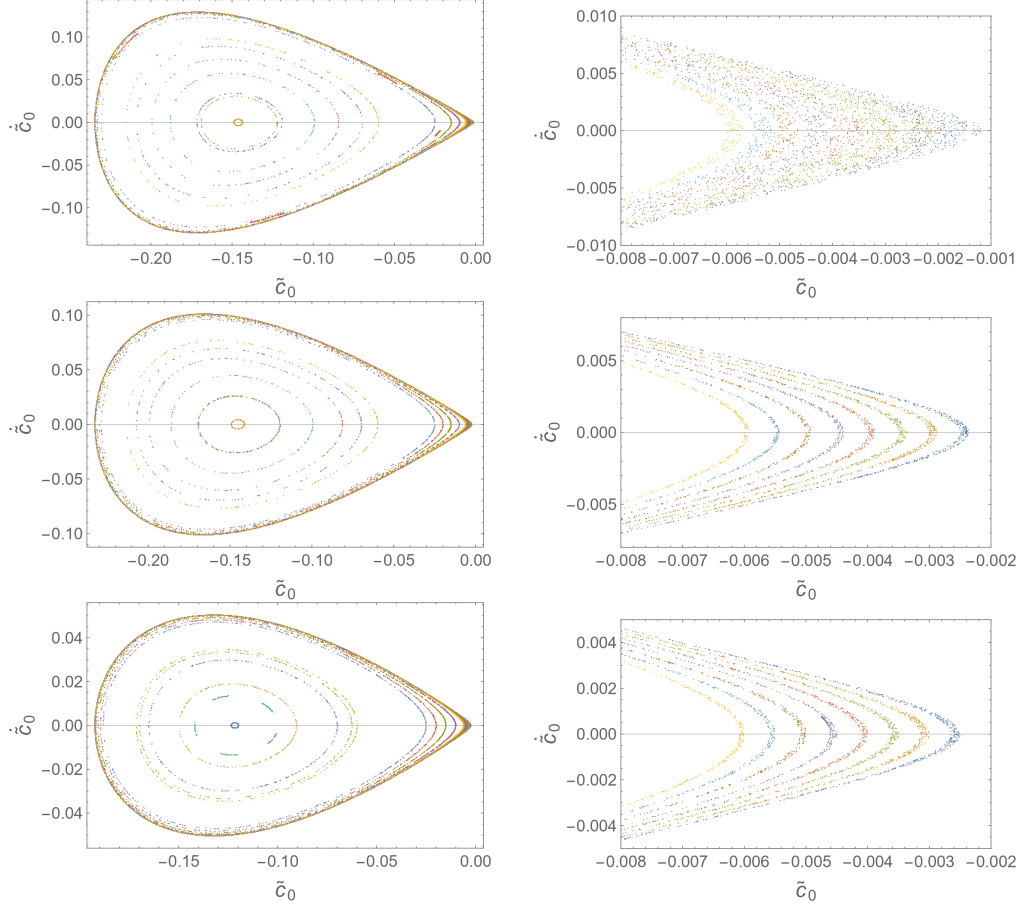


Figure 4: Poincaré sections for a time-dependent perturbed string, obtained changing the initial conditions, with $r_0 = 1.1$ and increasing the chemical potential $\mu = 0.3$ (top row), $\mu = 0.6$ (middle row) and $\mu = 0.9$ (bottom row), for $\tilde{c}_1 = 0$ and $\dot{\tilde{c}}_1 \geq 0$. The plots in the right column enlarge the corresponding ones in the left column in the range of small \tilde{c}_0 , $\dot{\tilde{c}}_0$.

In Fig. 5 we observe that when the string is along x_3 we go closer to $\tilde{c}_0 = 0$ to observe chaos. In the Poincaré plots we set $\tilde{c}_1 = 0$. In this case the potential has a trap for $\tilde{c}_0 < 0$. Considering the definition of the perturbation given in Eqs. (15) and (20), the perturbation characterized by $\tilde{c}_1 = 0$ and $\tilde{c}_0 < 0$, corresponding to $c_1 = 0$ and $c_0 < 0$, describes a string moving away from the event horizon. Therefore, for $(\tilde{c}_0, \tilde{c}_1) = (0, 0)$, hence for $(c_0, c_1) = (0, 0)$, the tip of the string is closest to the horizon.

We evaluate the Lyapunov exponents. In the four dimensional c_0, c_1 phase-space they can be computed for different values of μ or B using the numerical method described in [39]. A convergency plot is shown in Fig. 6, together with the sum of the Lyapunov exponents which converges to zero with the evolution.

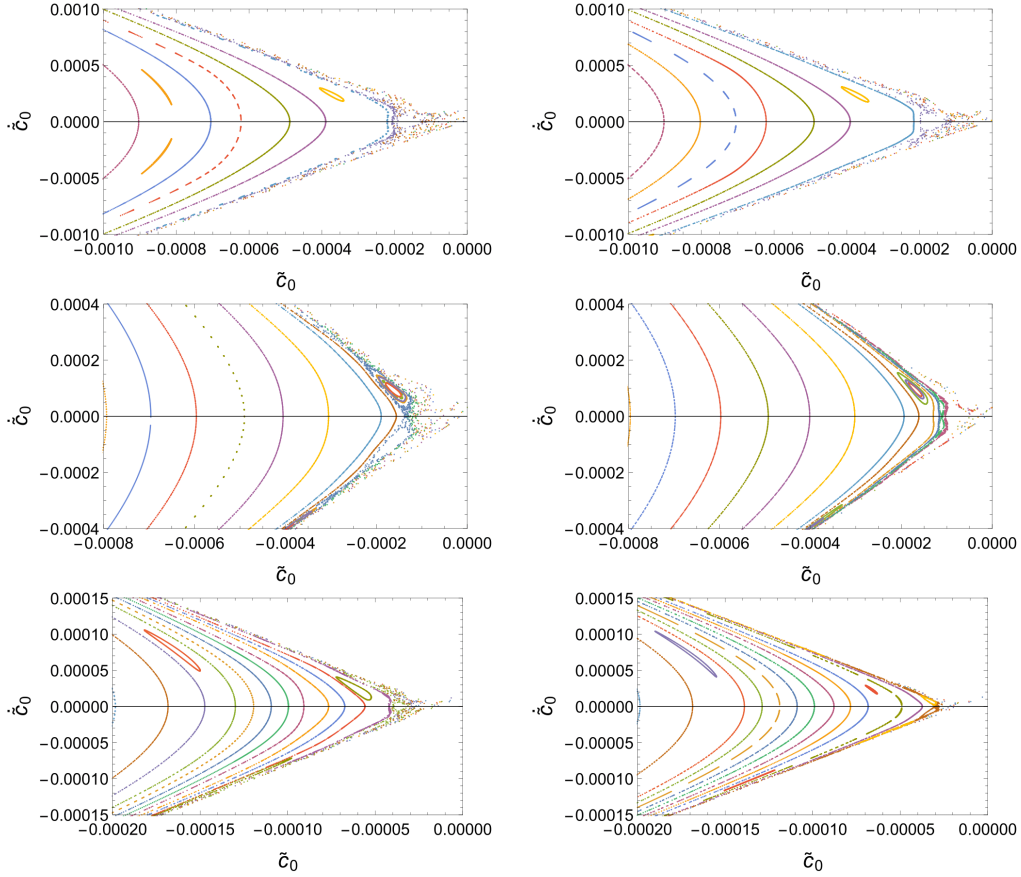


Figure 5: Poincaré sections for a perturbed string in the x_1 (left column) and x_3 configurations (right column). The initial conditions are changed with fixed energy $E = 10^{-5}$ and $r_0 = 1.1$. The magnetic field is increased from $B = 0.3$ (top row) to $B = 0.6$ (middle row) and $B = 1$ (bottom row). The sections correspond to $\tilde{c}_1 = 0$ and $\dot{\tilde{c}}_1 \geq 0$.

The convergency plot is a damped oscillating function. The value of the largest Lyapunov exponent can be extrapolated fitting the maximum in each oscillation and considering $t \rightarrow +\infty$. The values obtained decrease as μ or B increases, as shown in Fig. 7: the effect of the magnetic field and the chemical potential is to soften the dependence on the initial conditions, making the string less chaotic. At the right in Fig. 7 the results for the two configurations are compared. For the same values of B and r_0 , so at the same distance from the BH horizon, smaller Lyapunov exponents are found in the x_3 configuration. The Poincaré plots show that chaos is produced in the proximity of the BH horizon, and that the string dynamics is less chaotic if the chemical potential or the magnetic field increases. This is confirmed by the largest Lyapunov exponent. As we can see from the plots in Fig. 7, the MSS bound is satisfied for both the metrics, since $5/3 \leq \lambda_{MSS} \leq 2$

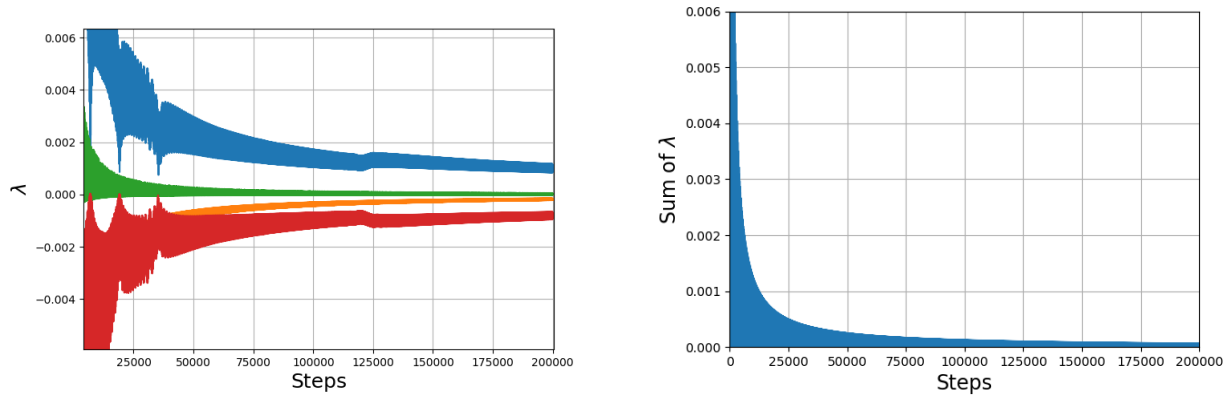


Figure 6: Left: convergency plot of the four Lyapunov exponents for a string along x_1 , with $r_0 = 1.1$ and $B = 0.6$. 2×10^5 time steps are shown. For the initial conditions, the energy is set to $E = 10^{-5}$ together with $\tilde{c}_0 = -0.0002$, $\dot{\tilde{c}}_0 = 0$, $\tilde{c}_1 = 0.0011$. Right: sum of the Lyapunov exponents for the same value of B .

and $0.56 \leq \lambda_{MSS} \leq 2$ for the two considered cases.

The AdS-RN metric in Eq. (41) can be modified with a warp factor, used to implement a confinement mechanism in holographic models of QCD [40]. The line element is defined as

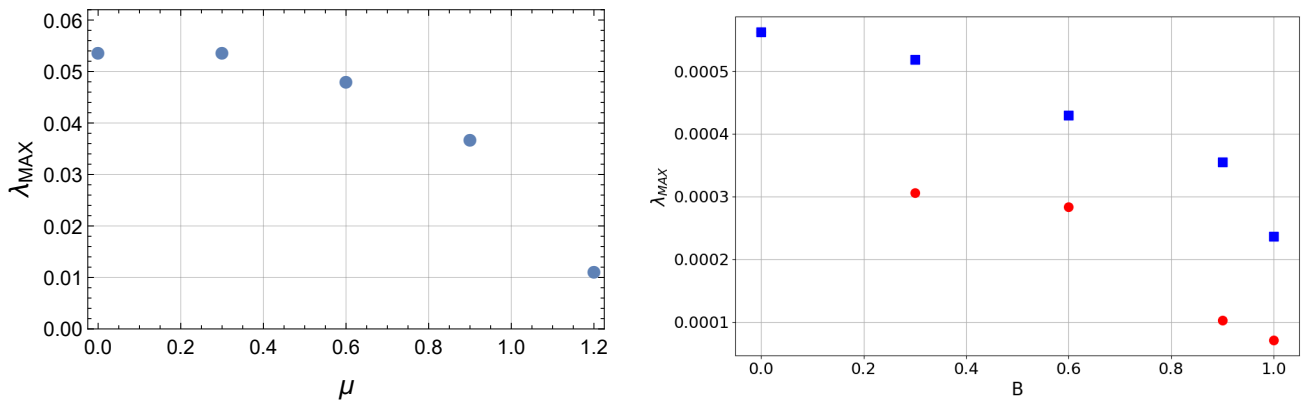


Figure 7: Largest Lyapunov exponent λ_{MAX} versus μ (left) and B (right) for $r_0 = 1.1$. In the plot at right the results for the x_1 (blue squares) and x_3 string configurations (red points) are shown.

$$ds^2 = e^{-\frac{c^2}{r^2}} \left(-f(r) r^2 dt^2 + r^2 d\mathbf{x}^2 + \frac{1}{r^2 f(r)} dr^2 \right), \quad (52)$$

with metric function $f(r)$ in (40). The Hawking temperature does not depend on the dilaton parameter c , therefore it is given in Eq. (42). The warp factor mainly affects the IR small r region, while the geometry became asymptotically AdS_5 in the UV $r \rightarrow \infty$ region. A dilaton factor has been used to study features of the QCD phenomenology at finite temperature and baryon density, namely the behaviour of the quark and gluon condensates increasing T and μ , the phase diagram, and the in-medium broadening of the spectral functions of two-point correlators [40–43]

To study the dependence on the dilaton parameter c , we inspect the Poincaré plots and compute the Lyapunov exponents. The Poincaré sections for $r_h = 1$, $r_0 = 1.1$, $\mu = 0$ at different c are shown in Fig. 8.

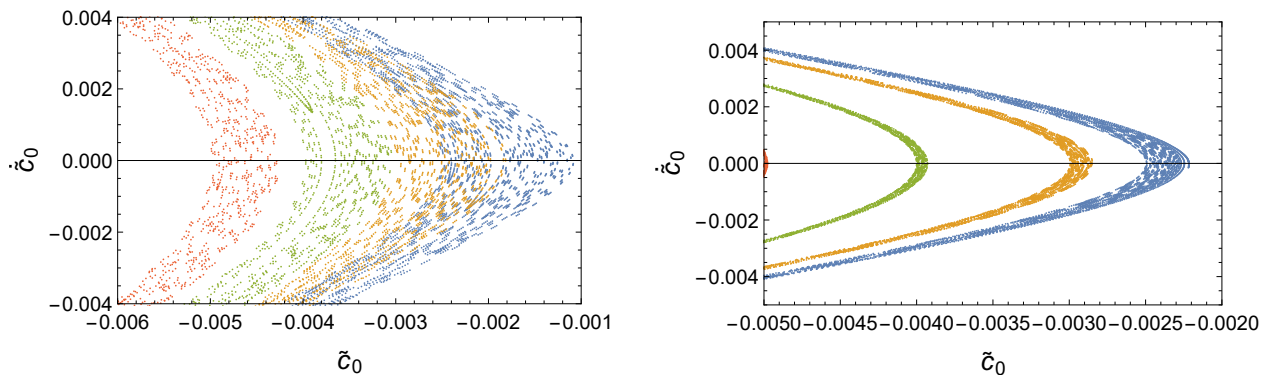


Figure 8: Zoom in the small \tilde{c}_0 , \dot{c}_0 region of the Poincaré section for the perturbed string in the background geometry with warp factor (52), for $r_0 = 1.1$, $\mu = 0$ and parameter of the dilaton $c = 1$ (left) and $c = 2$ (right). The sections are obtained setting the energy $E = 1 \times 10^{-5}$ and a time evolution of 8×10^{-3} time steps.

As we can see from the Poincaré section increasing the dilaton parameter stabilizes the system. This is confirmed by the maximum Lyapunov exponent as a function of c , Fig 9. The MSS bound is satisfied, since $\lambda_{MAX} \ll \lambda_{MSS} = 2$ for all values of the dilaton parameter c .

6 Conclusions

We have presented a method to explore the chaotic behaviour of a strongly coupled $Q\bar{Q}$ system at finite temperature through its gravity dual system. This allows us to test the Maldacena, Shenker and Stanford conjecture. Chaos has been observed in the Poincaré

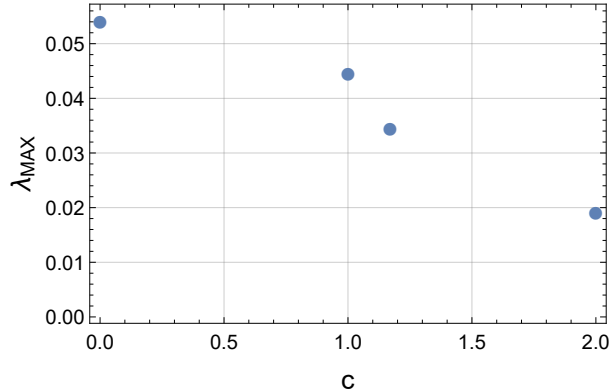


Figure 9: Largest Lyapunov exponent for $r_0 = 1.1$ and $\mu = 0$, increasing the dilaton constant.

plots, characterized by scattered points in the region close to the black hole horizon, and quantitatively described computing the Lyapunov exponents. The system becomes less chaotic increasing μ , B and c . For the magnetic field case, anisotropy effect in two different orientations of the string is found. The stabilization effect of the magnetic field is stronger for the configuration with string endpoints lying on a line parallel to the field. The MSS bound (1) is satisfied for the largest Lyapunov exponent and therefore, also the generalization (2). The MSS bound remains universal.

Acknowledgements. I thank P. Colangelo, F. De Fazio and F. Giannuzzi, co-authors of the works on which this review is based on. This study has been carried out within the INFN project (Iniziativa Specifica) QFT-HEP.

References

- [1] P. Colangelo, F. De Fazio, and N. Losacco, *Chaos in a $Q\bar{Q}$ system at finite temperature and baryon density*, *Phys. Rev. D* **102** (2020) 074016, [[arXiv:2007.06980](https://arxiv.org/abs/2007.06980)].
- [2] P. Colangelo, F. Giannuzzi, and N. Losacco, *Chaotic dynamics of a suspended string in a gravitational background with magnetic field*, *Phys. Lett. B* **827** (2022) 136949, [[arXiv:2111.09441](https://arxiv.org/abs/2111.09441)].
- [3] J. Maldacena, S. H. Shenker, and D. Stanford, *A bound on chaos*, *JHEP* **08** (2016) 106, [[arXiv:1503.01409](https://arxiv.org/abs/1503.01409)].

- [4] Y. Sekino and L. Susskind, *Fast Scramblers*, *JHEP* **10** (2008) 065, [[arXiv:0808.2096](#)].
- [5] L. Susskind, *Addendum to Fast Scramblers*, [arXiv:1101.6048](#).
- [6] S. H. Shenker and D. Stanford, *Black holes and the butterfly effect*, *JHEP* **03** (2014) 067, [[arXiv:1306.0622](#)].
- [7] S. H. Shenker and D. Stanford, *Stringy effects in scrambling*, *JHEP* **05** (2015) 132, [[arXiv:1412.6087](#)].
- [8] A. Kitaev, *Hidden correlations in the Hawking radiation and thermal noise*, *Breakthrough Prize Fundamental Physics Symposium, 11/10/2014, KITP seminar* (2014).
- [9] J. Polchinski, *Chaos in the black hole S-matrix*, [arXiv:1505.08108](#).
- [10] D. Giataganas, *Chaotic Motion near Black Hole and Cosmological Horizons*, [arXiv:2112.02081](#).
- [11] L. Susskind, *Why do Things Fall?*, [arXiv:1802.01198](#).
- [12] A. R. Brown, H. Gharibyan, A. Streicher, L. Susskind, L. Thorlacius, and Y. Zhao, *Falling Toward Charged Black Holes*, *Phys. Rev. D* **98** (2018) 126016, [[arXiv:1804.04156](#)].
- [13] J. M. Maldacena, *Wilson loops in large N field theories*, *Phys. Rev. Lett.* **80** (1998) 4859–4862, [[hep-th/9803002](#)].
- [14] E. Witten, *Anti-de Sitter space and holography*, *Adv. Theor. Math. Phys.* **2** (1998) 253, [[hep-th/9802150](#)].
- [15] S. Gubser, I. R. Klebanov, and A. M. Polyakov, *Gauge theory correlators from noncritical string theory*, *Phys. Lett. B* **428** (1998) 105–114, [[hep-th/9802109](#)].
- [16] J. de Boer, E. Llabrs, J. F. Pedraza, and D. Vegh, *Chaotic strings in AdS/CFT*, *Phys. Rev. Lett.* **120** (2018) 201604, [[arXiv:1709.01052](#)].
- [17] S. Dalui, B. R. Majhi, and P. Mishra, *Presence of horizon makes particle motion chaotic*, *Phys. Lett. B* **788** (2019) 486–493, [[arXiv:1803.06527](#)].
- [18] S. Dalui and B. R. Majhi, *Near horizon local instability and quantum thermality*, *Phys. Rev. D* **102** (2020) 124047, [[arXiv:2007.14312](#)].
- [19] D. S. Ageev, *Butterflies dragging the jets: on the chaotic nature of holographic QCD*, [arXiv:2105.04589](#).

- [20] D.-Z. Ma, F. Xia, D. Zhang, G.-Y. Fu, and J.-P. Wu, *Chaotic dynamics of string around the conformal black hole*, *Eur. Phys. J. C* **82** (2022), no. 4 372, [[arXiv:2205.00226](#)].
- [21] S. D. Avramis, K. Sfetsos, and K. Siampos, *Stability of strings dual to flux tubes between static quarks in $N = 4$ SYM*, *Nucl. Phys. B* **769** (2007) 44–78, [[hep-th/0612139](#)].
- [22] R. E. Arias and G. A. Silva, *Wilson loops stability in the gauge/string correspondence*, *JHEP* **01** (2010) 023, [[arXiv:0911.0662](#)].
- [23] C. Nunez, M. Piai, and A. Rago, *Wilson Loops in string duals of Walking and Flavored Systems*, *Phys. Rev. D* **81** (2010) 086001, [[arXiv:0909.0748](#)].
- [24] L. Bellantuono, P. Colangelo, F. De Fazio, F. Giannuzzi, and S. Nicotri, *Quarkonium dissociation in a far-from-equilibrium holographic setup*, *Phys. Rev. D* **96** (2017) 034031, [[arXiv:1706.04809](#)].
- [25] K. Hashimoto, K. Murata, and N. Tanahashi, *Chaos of Wilson Loop from String Motion near Black Hole Horizon*, *Phys. Rev. D* **98** (2018) 086007, [[arXiv:1803.06756](#)].
- [26] T. Ishii, K. Murata, and K. Yoshida, *Fate of chaotic strings in a confining geometry*, *Phys. Rev. D* **95** (2017) 066019, [[arXiv:1610.05833](#)].
- [27] T. Akutagawa, K. Hashimoto, K. Murata, and T. Ota, *Chaos of QCD string from holography*, *Phys. Rev. D* **100** (2019) 046009, [[arXiv:1903.04718](#)].
- [28] I. Halder, *Global Symmetry and Maximal Chaos*, [[arXiv:1908.05281](#)].
- [29] R. Critelli, R. Rougemont, S. I. Finazzo, and J. Noronha, *Polyakov loop and heavy quark entropy in strong magnetic fields from holographic black hole engineering*, *Phys. Rev. D* **94** (2016) 125019, [[arXiv:1606.09484](#)].
- [30] A. Ballon-Bayona, J. P. Shock, and D. Zoakos, *Magnetic catalysis and the chiral condensate in holographic QCD*, *JHEP* **10** (2020) 193, [[arXiv:2005.00500](#)].
- [31] I. Y. Aref’eva, K. Rannu, and P. Slepov, *Holographic model for heavy quarks in anisotropic hot dense QGP with external magnetic field*, *JHEP* **07** (2021) 161, [[arXiv:2011.07023](#)].
- [32] I. Y. Aref’eva, K. Rannu, and P. Slepov, *Energy Loss in Holographic Anisotropic Model for Heavy Quarks in External Magnetic Field*, [[arXiv:2012.05758](#)].

- [33] I. Y. Aref'eva, K. Rannu, and P. S. Slepov, *Anisotropic solutions for a holographic heavy-quark model with an external magnetic field*, *Teor. Mat. Fiz.* **207** (2021), no. 1 44–57.
- [34] I. Y. Aref'eva, A. Ermakov, K. Rannu, and P. Slepov, *Holographic model for light quarks in anisotropic hot dense QGP with external magnetic field*, [arXiv:2203.12539](https://arxiv.org/abs/2203.12539).
- [35] B. H. Lee, C. Park, and S. J. Sin, *A dual geometry of the hadron in dense matter*, *Journal of High Energy Physics* **2009** (Jul, 2009) 087–087.
- [36] E. D'Hoker and P. Kraus, *Magnetic Brane Solutions in AdS*, *JHEP* **10** (2009) 088, [[arXiv:0908.3875](https://arxiv.org/abs/0908.3875)].
- [37] E. D'Hoker and P. Kraus, *Charged Magnetic Brane Solutions in AdS (5) and the fate of the third law of thermodynamics*, *JHEP* **03** (2010) 095, [[arXiv:0911.4518](https://arxiv.org/abs/0911.4518)].
- [38] D. Li, M. Huang, Y. Yang, and P.-H. Yuan, *Inverse Magnetic Catalysis in the Soft-Wall Model of AdS/QCD*, *JHEP* **02** (2017) 030, [[arXiv:1610.04618](https://arxiv.org/abs/1610.04618)].
- [39] M. Sandri, *Numerical calculation of Lyapunov exponents*, *Mathematica Journal* **6** (1996), no. 3 78–84.
- [40] P. Colangelo, F. Giannuzzi, S. Nicotri, and F. Zuo, *Temperature and chemical potential dependence of the gluon condensate: a holographic study*, *Phys. Rev. D* **88** (2013), no. 11 115011, [[arXiv:1308.0489](https://arxiv.org/abs/1308.0489)].
- [41] P. Colangelo, F. Giannuzzi, and S. Nicotri, *Holography, Heavy-Quark Free Energy, and the QCD Phase Diagram*, *Phys. Rev. D* **83** (2011) 035015, [[arXiv:1008.3116](https://arxiv.org/abs/1008.3116)].
- [42] P. Colangelo, F. Giannuzzi, S. Nicotri, and V. Tangorra, *Temperature and quark density effects on the chiral condensate: An AdS/QCD study*, *Eur. Phys. J. C* **72** (2012) 2096, [[arXiv:1112.4402](https://arxiv.org/abs/1112.4402)].
- [43] P. Colangelo, F. Giannuzzi, and S. Nicotri, *In-medium hadronic spectral functions through the soft-wall holographic model of QCD*, *JHEP* **05** (2012) 076, [[arXiv:1201.1564](https://arxiv.org/abs/1201.1564)].